

# GRAVITATIONAL COLLAPSE OF A BROWNIAN GAS

CLÉMENT SIRE AND PIERRE-HENRI CHAVANIS

*Laboratoire de Physique Théorique (UMR 5152 du CNRS), Université Paul Sabatier,  
118, route de Narbonne, 31062 Toulouse Cedex 4, France  
E-mail: Clement.Sire@irsamc.ups-tlse.fr & Chavanis@irsamc.ups-tlse.fr*

**Abstract.** We investigate a model describing the dynamics of a gas of self-gravitating Brownian particles. This model can also have applications for the chemotaxis of bacterial populations. We focus here on the collapse phase obtained at sufficiently low temperature/energy and on the post-collapse regime following the singular time where the central density diverges. Several analytical results are illustrated by numerical simulations.

## 1. Introduction

The general study of the static and dynamical properties of a self-gravitating gas is a long standing problem in physics. Apart for its clear applications in astrophysics, this problem has also many conceptual interests, as for instance, the non-equivalence of thermodynamical ensembles for many-body systems with long range interactions [17].

In this paper, instead of considering the self-gravitating Newtonian gas (*i.e.* obeying Newton's equations), we study a gas of self-gravitating Brownian particles [10] subject to a friction originating from the presence of an inert gas and to a stochastic force (modeling turbulent fluctuations, collisions,...). This system has a rigorous canonical structure where the temperature  $T$  measures the strength of the stochastic force. Thus, we can precisely check the thermodynamical predictions of Kiessling [14] and Chavanis [5] obtained in the canonical ensemble.

For long-range interacting systems, the mean-field approximation is presumed to become exact if the thermodynamical limit is taken properly. In a strong friction limit (or for large times), the self-gravitating Brownian gas reduces to the Smoluchowski-Poisson system, that is a Fokker-Planck equation describing the particle density evolution in the presence of a gravitational field  $\Phi$ , coupled self-consistently to Poisson's equation, stating that the gravitational field is created by the gas itself.

---

2000 *Mathematics Subject Classification:*

*Key words and phrases:* Gravitational collapse.

The paper is in final form and no version of it will be published elsewhere.

This set of equations conserves mass and decreases the Boltzmann free energy [6]. They describe the competition between the gravitational force which favors a collapsed state and the kinetic pressure/diffusion/temperature which tends to spread the particles over the entire accessible space. It is thus expected that below a certain critical temperature  $T_c$ , the system undergoes a situation of “isothermal collapse” [5], which is the canonical version of the “gravothermal catastrophe” [15]. These equations have not been considered by astrophysicists because the canonical ensemble is not the correct description of stellar systems and usual astrophysical bodies do not experience a friction with a gas (except dust particles in the solar nebula [3]). Yet, it is clear that the self-gravitating Brownian gas model is of considerable conceptual interest in statistical mechanics to understand the strange thermodynamics of systems with long-range interactions and the inequivalence of statistical ensembles. In addition, it provides one of the first model of stochastic particles with long-range interactions, thereby extending the classical Einstein-Smoluchowski model [18] to a more general context [6].

In addition, it turns out that the same type of equations occurs in biology in relation with the chemotactic aggregation of bacterial populations [16]. A general model of chemotactic aggregation has been proposed by Keller & Segel [13] in the form of two coupled partial differential equations. In some approximation, this model reduces to the Smoluchowski-Poisson system [10]. Non-local drift-diffusion equations analogous to the Smoluchowski-Poisson system have also been introduced in two-dimensional hydrodynamics in relation with the formation of large-scale vortices such as Jupiter’s great red spot [19, 11, 4]. These analogies, developed in [6, 9], give further physical interest to our Brownian model.

We now introduce a continuous mass density  $\rho(\mathbf{r})$  in a sphere a radius  $R$ , and define respectively

- Total mass:  $M = \int \rho(\mathbf{r}) d^D r$
- Energy:  $E = \frac{D}{2}MT + \frac{1}{2} \int \rho(\mathbf{r})\Phi(\mathbf{r}) d^D r$
- Entropy:  $S = \frac{D}{2}M \ln T - \int \rho(\mathbf{r}) \ln[\rho(\mathbf{r})] d^D r$

At equilibrium, the gravitational potential is given by the Boltzmann-Poisson equation:

$$\Delta\Phi(\mathbf{r}) = S_D G \rho(\mathbf{r}), \quad (1)$$

$$\rho(\mathbf{r}) = \frac{1}{Z} \exp[-\beta\Phi(\mathbf{r})], \quad (2)$$

where  $\Phi$  is the gravitational potential,  $S_D$  is the surface of the unit  $D$ -dimensional sphere, and  $Z$  is the normalization (partition function). Note that these equations would be the same for a Newtonian gas in the mean-field limit, as Eq. (2) simply states that the density is given by the Boltzmann weight. The microcanonical version of this model can be defined by imposing the total energy  $E$  instead of the temperature  $T$ . Although the equilibrium distributions are the same, the stability limits differ in microcanonical (fixed  $E$ ) and canonical (fixed  $T$ ) ensembles [5]. A typical phase diagram is displayed in Fig. 1 (for  $D = 3$ ). This illustrates the fact that at low enough temperature in the canonical

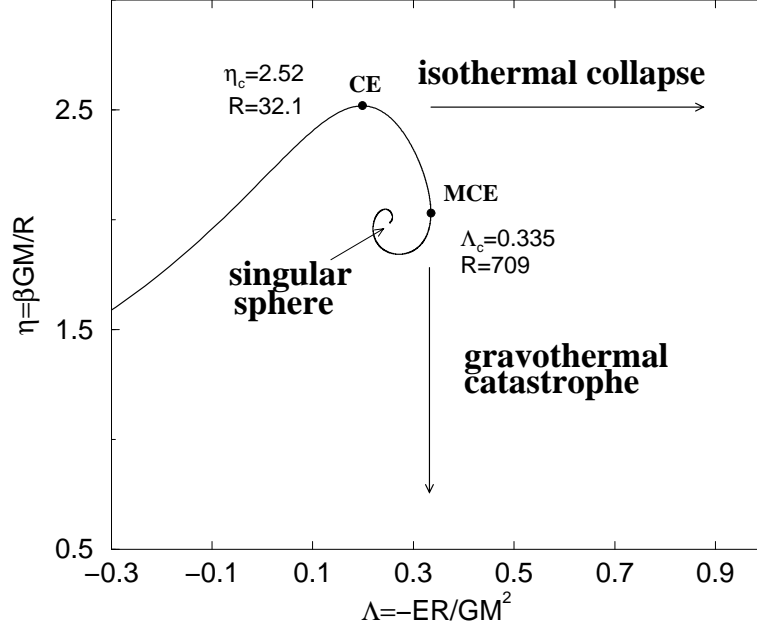


Figure 1: We show the phase diagram of a self-gravitating Brownian gas in  $D = 3$ . In the canonical ensemble, there is no equilibrium state below the rescaled temperature  $T_c = \eta_c^{-1} \approx 0.396$ , whereas in the microcanonical ensemble, the system collapses below the rescaled energy  $E_c = -\Lambda_c \approx -0.335$ . The equilibrium phase diagram in all dimensions  $D$ , as well as for Langevin particles obeying Tsallis statistics has been studied in [20, 7].

ensemble, the system does not have any equilibrium state, whereas the same situation arises in the microcanonical ensemble at low enough energy. The static phase diagram and the detailed stability analysis of the solutions have been extensively studied in [20, 7] for isothermal and polytropic distributions and for any dimension of space.

In this paper, we focus on the dynamical properties of the system when no equilibrium state exists. In section 2, after stating the problem, we study scaling collapse solutions in the canonical ensemble (for  $D \geq 2$ , including the critical case  $D = 2$ ) and in the microcanonical ensemble (for  $D > 2$ ). In both cases, the central density diverges in a finite time  $t_{coll}$  (except in  $D = 2$  for  $T = T_c$  at which  $t_{coll} \rightarrow +\infty$ ). In section 3, we show that the singular state reached at  $t_{coll}$ , which does not coincide with the condensed state predicted by statistical mechanics [14, 5], is indeed not the final stage of the dynamics. We then study the post-collapse stage, which is characterized by the creation of a Dirac peak and the existence of a backward scaling dynamics regime. Finally, we illustrate the very large time regime where a dilute gas of Brownian particles evolves around a massive core.

## 2. Collapse dynamics of self-gravitating Brownian particles

- *Dynamics of the Smoluchowski-Poisson system*

At a given temperature  $T$  controlling the diffusion coefficient, the density  $\rho(\mathbf{r}, t)$  of a system of self-gravitating Brownian particles satisfies the following coupled equations:

$$\frac{\partial \rho}{\partial t} = \nabla \left[ \frac{1}{\xi} (\mathcal{D} \nabla \rho + \rho \nabla \Phi) \right], \quad (3)$$

$$\Delta \Phi = S_D G \rho, \quad (4)$$

where  $\mathcal{D}$  is a diffusion constant. In the present paper, we will consider  $\mathcal{D} = T$  consistently with Einstein's relation. We thus have to solve the Smoluchowski-Poisson system. At equilibrium, implying a vanishing current, these equations simply reduce to Eq. (1-2).

The more general case where  $\mathcal{D}$  is a function of  $\rho$  itself can also be of interest [6]. For example, by taking  $\mathcal{D}(\rho) \sim \rho^{1/n}$ , one describes a gas of self-gravitating Langevin particles displaying anomalous diffusion [7]. The static properties of this system reproduce that of a gravitational gas described by Tsallis statistics. The equilibrium distributions correspond to polytropes which are associated with the  $q$ -entropy  $S_q = -\frac{1}{q-1} \int (f^q - f) d^D \mathbf{r} d^D \mathbf{v}$ , where  $f(\mathbf{r}, \mathbf{v})$  is the phase space density. The parameters  $q$  and  $n$  are related to each other by the relation

$$n = \frac{D}{2} + \frac{1}{q-1}. \quad (5)$$

This system can have self-confined equilibrium states depending on  $n$  and  $D$ . It can also undergo gravitational collapse at sufficiently low temperature/energy as illustrated on Fig. 2 (lower curve).

From now on, we take  $\mathcal{D} = T$  and set  $M = R = G = \xi = 1$ . We shall also restrict ourselves to spherically symmetric solutions. The equations of the problem then become

$$\frac{\partial \rho}{\partial t} = \nabla (T \nabla \rho + \rho \nabla \Phi), \quad (6)$$

$$\Delta \Phi = S_D \rho, \quad (7)$$

with proper boundary conditions in order to impose a vanishing particle flux on the surface of the confining sphere. These read

$$\frac{\partial \Phi}{\partial r}(0, t) = 0, \quad \Phi(1) = \frac{1}{2-D}, \quad T \frac{\partial \rho}{\partial r}(1) + \rho(1) = 0, \quad (8)$$

for  $D > 2$ . For  $D = 2$ , we take  $\Phi(1) = 0$  on the boundary. Integrating Eq. (7) once, we can rewrite the Smoluchowski-Poisson system in the form of a single integrodifferential equation

$$\frac{\partial \rho}{\partial t} = \frac{1}{r^{D-1}} \frac{\partial}{\partial r} \left\{ r^{D-1} \left( T \frac{\partial \rho}{\partial r} + \frac{\rho}{r^{D-1}} \int_0^r \rho(r') S_D r'^{D-1} dr' \right) \right\}. \quad (9)$$

The Smoluchowski-Poisson system is also equivalent to a single differential equation

$$\frac{\partial M}{\partial t} = T \left( \frac{\partial^2 M}{\partial r^2} - \frac{D-1}{r} \frac{\partial M}{\partial r} \right) + \frac{1}{r^{D-1}} M \frac{\partial M}{\partial r}, \quad (10)$$

for the quantity

$$M(r, t) = \int_0^r \rho(r') S_D r'^{D-1} dr', \quad (11)$$

which represents the mass contained within the sphere of radius  $r$ . The appropriate boundary conditions are

$$M(0, t) = N_0(t), \quad M(1, t) = 1, \quad (12)$$

where  $N_0(t) = 0$ , except if the density develops a condensed Dirac peak contribution at  $r = 0$ , of total mass  $N_0(t)$ . It is also convenient to introduce the function  $s(r, t) = M(r, t)/r^D$  satisfying

$$\frac{\partial s}{\partial t} = T \left( \frac{\partial^2 s}{\partial r^2} + \frac{D+1}{r} \frac{\partial s}{\partial r} \right) + \left( r \frac{\partial s}{\partial r} + Ds \right) s. \quad (13)$$

- *Self-similar solutions of the Smoluchowski-Poisson system in  $D > 2$*

In [10, 20, 7], we have shown that in the canonical ensemble (fixed  $T$ ), the system undergoes gravitational collapse below a critical temperature  $T_c$  depending on the dimension of space. The density develops a scaling profile, and the central density grows and diverges at a finite time  $t_{coll}$ .

We look for self-similar solutions of the form

$$\rho(r, t) = \rho_0(t) f\left(\frac{r}{r_0(t)}\right), \quad r_0 = \left(\frac{T}{\rho_0}\right)^{1/2}, \quad (14)$$

where the King's radius  $r_0$  defines the size of the dense core [2]. In terms of the mass profile, we have

$$M(r, t) = M_0(t) g\left(\frac{r}{r_0(t)}\right), \quad \text{with} \quad M_0(t) = \rho_0 r_0^D, \quad (15)$$

and

$$g(x) = S_D \int_0^x f(x') x'^{D-1} dx'. \quad (16)$$

In terms of the function  $s$ , we have

$$s(r, t) = \rho_0(t) S\left(\frac{r}{r_0(t)}\right), \quad \text{with} \quad S(x) = \frac{g(x)}{x^D}. \quad (17)$$

Substituting the *ansatz* (17) into Eq. (13), we find that

$$\frac{d\rho_0}{dt} S(x) - \frac{\rho_0}{r_0} \frac{dr_0}{dt} x S'(x) = \rho_0^2 \left( S''(x) + \frac{D+1}{x} S'(x) + x S(x) S'(x) + D S(x)^2 \right), \quad (18)$$

where we have set  $x = r/r_0$ . The variables of position and time separate provided that  $\rho_0^{-2} d\rho_0/dt$  is a constant that we arbitrarily set equal to 2. After time integration, this leads to

$$\rho_0(t) = \frac{1}{2}(t_{coll} - t)^{-1}, \quad (19)$$

so that the central density becomes infinite in a finite time  $t_{coll}$ , which appears as a integration constant. The scaling equation now reads

$$2S + xS' = S'' + \frac{D+1}{x} S' + S(xS' + DS). \quad (20)$$

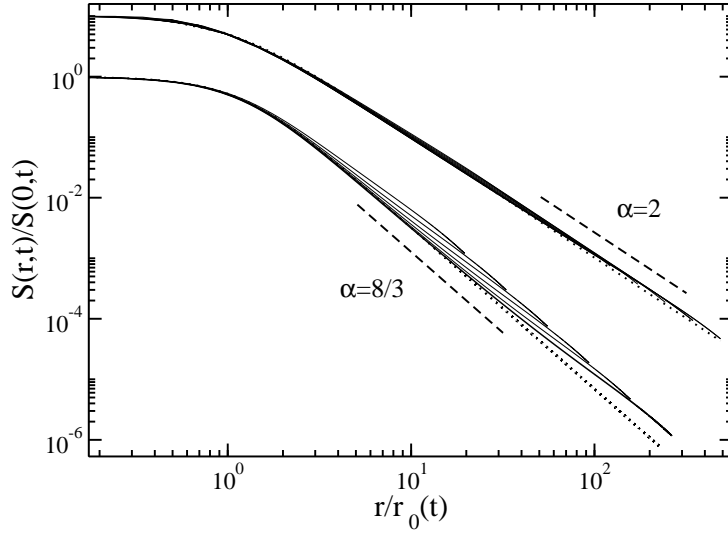


Figure 2: In  $D = 3$ , we plot  $s(r,t)/s(0,t)$  as a function of  $r/r_0(t)$  for different times (density range  $10^2 - 10^7$ ). The upper curve corresponds to a constant diffusion coefficient  $\mathcal{D} = T$ , i.e.  $n = \infty$ , leading to  $\alpha = 2$  [10, 20]. The lower curve corresponds to  $\mathcal{D} \sim \rho^{1/n}$  leading to  $\alpha = \frac{2n}{n-1}$  (the numerical simulations corresponds to  $n = 4$ , hence  $\alpha = 8/3$ ) [7]. We compare the numerics to the analytical scaling solutions (dashed lines).

For  $D > 2$ , the scaling solution of Eq. (20) was obtained analytically in [20] and reads

$$S(x) = \frac{4}{D - 2 + x^2}, \quad (21)$$

which decays with an exponent  $\alpha = 2$ . This leads to (see Fig. 2, upper curve)

$$f(x) = \frac{4(D-2)}{S_D} \frac{x^2 + D}{(D-2+x^2)^2}, \quad g(x) = \frac{4x^D}{D-2+x^2}. \quad (22)$$

Note finally that within the core radius  $r_0$ , the total mass in fact vanishes as  $t \rightarrow t_{coll}$ . Indeed, from Eq. (15), we obtain

$$M(r_0(t), t) \sim \rho_0(t)r_0^D(t) \sim T^{D/2}(t_{coll} - t)^{D/2-1}. \quad (23)$$

Therefore, the collapse does *not* create a Dirac peak (“black hole”).

Near  $T_c$ , we find  $t_{coll} \sim (T_c - T)^{-1/2}$ , which is well supported by numerical simulations [10] and by a systematic expansion procedure performed in [8]. In addition, the width of the scaling regime is  $\delta t \sim (T_c - T)^{1/2}$ . This is an estimate of the time  $t_{coll} - \delta t$  from where the system enters the scaling regime. Above  $T_c$ , the equilibration time characterizing the exponential convergence to the stationary solution diverges like  $\tau \sim (T - T_c)^{-1/2}$  [8].

In [20], we have also studied the collapse dynamics at  $T = 0$  for which we obtained

$$\rho_0(t) \sim S_D^{-1}(t_{coll} - t)^{-1}, \quad (24)$$

as previously, but the core radius is not given anymore by the King's radius which vanishes for  $T = 0$ . Instead, we find

$$r_0 \sim \rho_0^{-1/\alpha}, \quad (25)$$

with

$$\alpha = \frac{2D}{D+2}. \quad (26)$$

The scaling function  $S(x)$  is only known implicitly

$$\left[ \frac{2}{D+2} - S(x) \right]^{\frac{D}{D+2}} = Kx^{\frac{2D}{D+2}} S(x), \quad (27)$$

where  $K$  is a known constant (see [20] for details),  $S(0) = \frac{2}{D+2}$ , and the large  $x$  asymptotics  $S(x) \sim f(x) \sim x^{-\alpha}$ . The mass within the core radius is now

$$M(r_0(t), t) \sim \rho_0(t)r_0^D(t) \sim (t_{coll} - t)^{D/2}, \quad (28)$$

and it again tends to zero as  $t \rightarrow t_{coll}$ . Comparing Eq. (23) and Eq. (28) suggests that if the temperature is very small, an apparent scaling regime corresponding to the  $T = 0$  case will hold up to a cross-over time  $t_*$ , with

$$t_{coll} - t_* \sim T^{D/2}. \quad (29)$$

Above  $t_*$ , the  $T \neq 0$  scaling ultimately prevails.

- *Scaling and “Pseudo-Scaling” solutions in  $D = 2$*

We now consider the critical dimension  $D = 2$  [20]. Above  $T_c = 1/4$ , the stationary solution can be explicitly computed, and the integrated mass is found to be

$$M(r) = \frac{4T}{4T-1} \frac{r^2}{1 + \frac{r^2}{4T-1}}. \quad (30)$$

Note that  $M(1) = 1$ , ensuring that the whole mass is included in this solution. Using  $\rho = \pi^{-1}dM/d(r^2)$ , we find that the density profile is given by

$$\rho(r) = \frac{4\rho_0}{\pi} \frac{1}{(1 + (r/r_0)^2)^2}, \quad (31)$$

with

$$r_0 = \sqrt{4T-1} \quad \text{and} \quad \rho_0 r_0^2 = T. \quad (32)$$

Note that the value of  $T_c$  and the dependence of  $r_0$  and  $\rho_0$  with the temperature coincide with the exact results obtained within conformal field theory [1].

We now set the temperature to be exactly  $T_c = 1/4$ . We then define  $a(t)$  in terms of the central density

$$\rho(0, t) = \frac{a(t) + 1}{\pi}. \quad (33)$$

The central density  $\rho(0, t)$  is expected to diverge for  $t \rightarrow +\infty$ , so that  $a(t)$  is also expected to diverge. Looking for a scaling solution for  $M(r, t)$ , we find that the scaling function coincides with the expression of the stationary solution of Eq. (30) and Eq. (31). More precisely, we find (see Fig. 3)

$$M(r, t) = \frac{a(t)r^2}{1 + a(t)r^2} + a(t)^{-1}h(r, t), \quad (34)$$

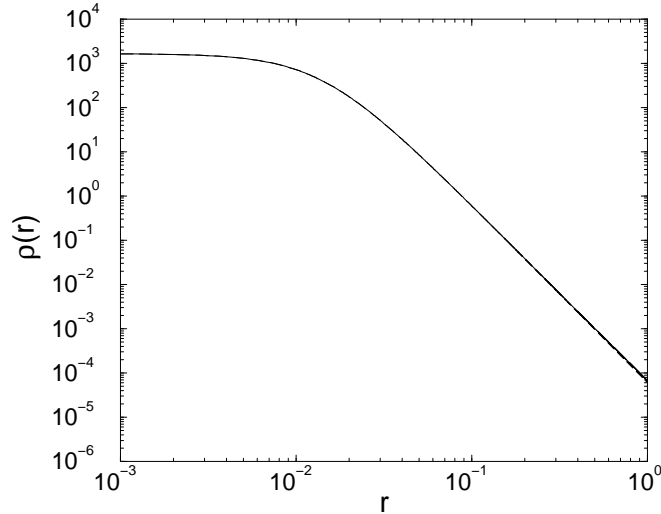


Figure 3: At  $T = T_c = 1/4$ , and when the central density has reached the value  $\rho(0, t) \approx 1644.8\dots = \frac{a(t)+1}{\pi}$  ( $a(t) \approx 5166.3\dots$ ), we have plotted the result of the numerical calculation compared to our exact scaling form  $\rho(r, t) = \frac{a(t)+1}{\pi}(1 + a(t)r^2)^{-2}$  (dashed line). The two curves are almost indistinguishable as the relative error is, as predicted, of order  $a^{-1} \sim 10^{-4}$ .

where  $h(r, t)$  can also be computed perturbatively in  $a^{-1}$  [20]. The introduction of the next correction to scaling is essential, as it governs the behavior of  $a(t)$ . Finally, one obtains

$$\frac{da}{dt} = \frac{a}{\ln a - 5/2} [1 + O(\ln a^{-2})], \quad (35)$$

leading to the asymptotic behavior

$$a(t) = \exp\left(\frac{5}{2} + \sqrt{2t}\right) [1 + O(t^{-1/2} \ln t)], \quad (36)$$

and a similar behavior for the density according to Eq. (33), which is in perfect agreement with numerical simulations [20]. Note that at  $T = T_c$  the central density does not diverge in a finite time  $t_{coll}$ .

Strictly below  $T_c$ , the scaling equation of Eq. (18) does not have any global physical solution. However, we find that by writing

$$M(r, t) = \frac{T}{T_c} \frac{a(t)r^2}{1 + a(t)r^2} + M_{cor}(r, t), \quad (37)$$

the correction  $M_{cor}(r, t)$  adiabatically satisfies an effective scaling relation of the form

$$M_{cor}(r, t) = a(t)^{\alpha/2-1} h_{cor}(\sqrt{a(t)}r), \quad (38)$$

where  $h_{cor}(x) \sim x^{2-\alpha}$ , for large  $x$ . Hence, the correction to the density scaling function satisfies  $\rho_{cor}(x) \sim x^{-\alpha}$ . The index  $\alpha$  is a very slowly varying function of time, such



that its explicit dependence on time does not affect the scaling equation for  $h_{cor}(x)$  or  $\rho_{cor}(x)$  [20]. Although the solution is not strictly speaking a true scaling solution, the explicit dependence of  $\alpha$  on  $a(t)$  is so weak that an apparent scaling should be seen with an effective  $\alpha$  almost constant for a wide range of values of  $a(t)$  or density. Hence, the total density profile is the sum of the scaling profile obtained at  $T_c$  with a  $T/T_c$  weight (behaving as a Dirac peak of weight  $T/T_c$  at  $t = t_{coll}$ , as  $\rho(r) \sim r^{-\alpha_c}$ , with  $\alpha_c = 4 > D = 2$ ) and of a pseudo-scaling solution associated to an effective scaling exponent slowly converging to  $\alpha = 2$ . More explicitly, we find [20]

$$2 - \alpha(t) = 2\sqrt{\frac{\ln \ln a}{2 \ln a}} (1 + O([\ln \ln a]^{-1})). \quad (39)$$

Let us illustrate quantitatively the time dependence of  $\alpha$ . For example, Eq. (39) respectively leads to  $\alpha(a = 10^3) = 1.27\dots$ , and to  $\alpha(a = 10^5) = 1.34\dots$ . Thus, for the typical values of  $a(t)$  accessible numerically of order  $a \sim 10^5$ , we expect to observe an apparent scaling solution with  $\alpha \approx 1.3$ . This is confirmed by the scaling plot of Fig. 4.

Finally, for  $T < T_c$ , we note that the central density diverges again in a finite time as one has

$$\frac{da}{dt} \sim a(t)^{1 + \frac{\alpha(t)}{2}}, \quad (40)$$

implying

$$\ln \rho_0(t) \sim -\ln(t_{coll} - t) \left[ 1 + \sqrt{-\frac{\ln |\ln(t_{coll} - t)|}{2 \ln(t_{coll} - t)}} + \dots \right]. \quad (41)$$

- *Scaling solutions in the microcanonical ensemble ( $D > 2$ )*

A microcanonical ensemble dynamics can be defined formally by considering Eq. (6) with a uniform but time dependent temperature  $T(t)$  such that the total energy is kept strictly constant. The resulting equations increase the Boltzmann entropy and display a sort of “gravothermal catastrophe” [10].

If one looks for a scaling solution, one still has  $\rho_0(t)r_0^2(t) = T(t)$ , but as the temperature is not necessarily asymptotically constant near  $t = t_{coll}$ , the exponent  $\alpha$  characterizing the decay of the density scaling function is not determined by simple dimensional analysis. In Ref. [10], we found numerically that the scaling equation Eq. (20) has physical solutions only for  $\alpha \leq \alpha_{max}$ , with  $\alpha_{max} \simeq 2.209\dots$  for  $D = 3$ . We also argued that the system will select the exponent  $\alpha_{max}$ , since it leads to the maximum increase of entropy. This is illustrated on Fig. 5, where the scaling collapse is plotted assuming respectively  $\alpha = 2$  and  $\alpha = \alpha_{max}$ . Note that if  $\alpha > 2$ , the temperature diverges at  $t = t_{coll}$ , as  $T(t) \sim \rho_0(t)^{1-2/\alpha}$ . However, in our most recent simulations (and this was confirmed by Guerra *et al.* [12]), we find that as one approaches  $t_{coll}$ , the temperature ultimately saturates to a finite value implying  $\alpha = 2$ . This can be understood by observing that the conservation of energy implies that if the temperature diverges, then the potential gravitational energy should also diverge. However, if  $\alpha < 5/2$  (in  $D = 3$ ), it is straightforward to show that the potential energy remains bounded. This exemplifies one of the inherent flaws of a model for which the temperature is maintained uniform, as we expect more

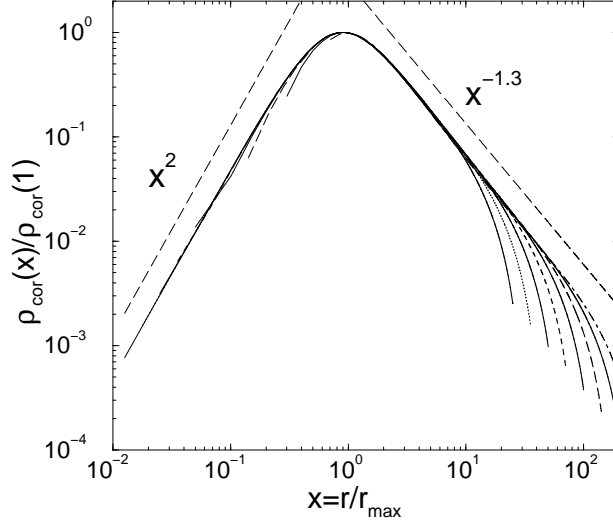


Figure 4: At  $T = T_c/2 = 1/8$ , we have extracted the next correction to scaling  $\rho_{\text{cor}} = \rho - T/T_c \rho_{T=T_c}$ . We have then plotted  $\rho_{\text{cor}}(r, t)/\rho_{\text{cor}}(r_{\text{max}}(t), t)$  as a function of  $x = r/r_{\text{max}}(t)$ , where  $r_{\text{max}}(t)$  is defined as the location of the maximum of  $\rho_{\text{cor}}(r, t)$ . Consistently with the apparent scaling observed, we found  $r_{\text{max}}^{-1}(t) \sim \sqrt{a} \sim \sqrt{\rho_{\text{cor}}(r_{\text{max}}(t), t)}$ . For  $a = 2^{n-1} \times 100$  ( $n = 1, \dots, 8$ ), we have obtained a convincing data collapse associated to  $\alpha \approx 1.3$ , in agreement with the theoretical estimate for  $\alpha$ , in this range of  $a$ .

realistically the temperature to grow in the dense core (containing a vanishing mass according to Eq. (23)), while remaining finite in the halo. We have shown [7] that in a more realistic model where  $T = T(r, t)$  is not necessarily uniform, by a phenomenon similar to the one leading to solutions for  $\alpha \in [2; \alpha_{\text{max}}]$ , the dynamics now selects a unique  $\alpha > 2$ .

As the existence of solutions of Eq. (18) for  $\alpha > 2$  is interesting and has physical implications in a more realistic model with a non uniform temperature, let us mention some analytical results about it. In the limit of large dimensions, the scaling equation can be perturbatively solved (in powers of  $D^{-1}$ ).

Defining  $z = \frac{DS(0)}{2}$  (which is of order  $O(1)$ ), and

$$x_0^2 = D + \frac{4}{z} + O(D^{-1}), \text{ or } x_0 = \sqrt{D} \left( 1 + \frac{2}{zD} + O(D^{-2}) \right), \quad (42)$$

such that  $S(x_0) = \alpha/D$ , and introducing

$$x_1^2 = \frac{D}{z-1} + \frac{2(z-2)}{z(z-1)} + O(D^{-1}), \quad (43)$$

we have obtained the explicit form for the scaling function up to second order in  $D^{-1}$  [20]

$$S(x) = \frac{\alpha}{D} \left[ 1 + \left( 1 - \frac{\alpha}{2z} \right) \left( \frac{x^2}{x_0^2} - 1 \right) \left( \frac{x^2}{x_1^2} + 1 \right)^{\frac{\alpha}{2}-1} \right]^{-1}. \quad (44)$$

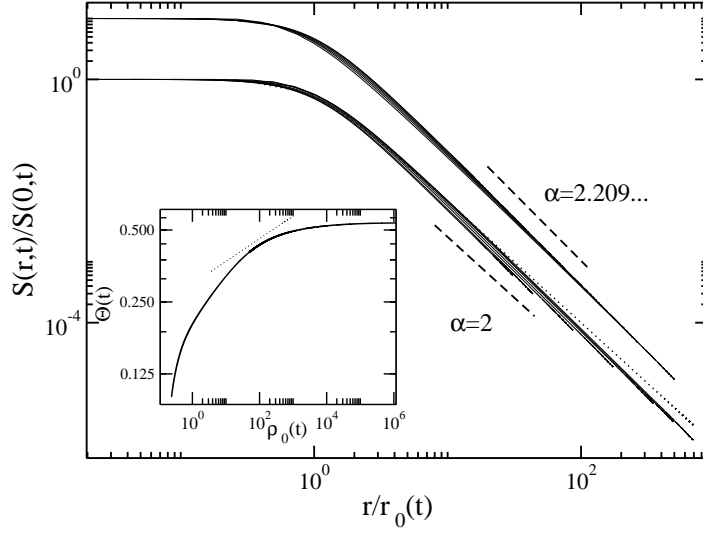


Figure 5: We plot  $s(r,t)/s(0,t)$  as a function of  $r/r_0(t)$  where  $r_0(t) \sim \rho_0(t)^{1/\alpha}$ . We try both values  $\alpha = 2$  and  $\alpha = \alpha_{\max} = 2.209733\dots$ , and compare both data collapses to the associated scaling function (dotted lines). The scaling associated to  $\alpha_{\max}$  is clearly more convincing than that for  $\alpha = 2$  (the two sets of curves have been shifted for clarity). However, our simulations also suggest that  $T(t) \sim \rho_0(t)^{1-2/\alpha_{\max}}$  does not diverge at  $t_{\text{coll}}$  (see the insert where a line of slope  $1 - 2/\alpha_{\max} \approx 0.09491\dots$  has been drawn), so that the asymptotic scaling should correspond to  $\alpha = 2$  (see also Guerra *et al.* [12]).

The scaling exponent  $\alpha$  is itself a function of  $S(0)$  (or  $z$ ), defined by

$$\alpha - 2 = \frac{4}{D} \left[ \frac{1}{z} - \frac{2}{z^2} \right] + \frac{8}{D^2} \left[ \frac{5}{z} - \frac{26}{z^2} + \frac{31}{z^3} - \frac{6}{z^4} - \left( \frac{1}{z} - \frac{7}{z^2} + \frac{14}{z^3} - \frac{8}{z^4} \right) \ln z \right] + O(D^{-3}). \quad (45)$$

This function has a well defined maximum for

$$z = \frac{D}{2} S(0) = 4 + \left( \frac{41}{2} - 6 \ln 2 \right) D^{-1} + O(D^{-2}), \quad (46)$$

associated to the value

$$\alpha_{\max} = 2 + \frac{1}{2} D^{-1} + \frac{11}{16} D^{-2} + O(D^{-3}). \quad (47)$$

This expansion gives  $\alpha_{\max} = 2.24\dots$  in  $D = 3$ , in fair agreement with the exact value  $\alpha_{\max} = 2.2097\dots$  obtained numerically in [10]. In addition, the exponent  $\alpha = 2$  is associated to  $z = DS(0)/2 = 2 + 4D^{-1} + O(D^{-2})$ , which coincides with the exact value  $S(0) = 4/(D-2)$  obtained in Eq. (21).

### 3. Post-collapse dynamics in the canonical ensemble

- *Post-collapse scaling at  $T = 0$*

According to general results of statistical mechanics [14, 5], the equilibrium state of self-gravitating particles in the canonical ensemble is a Dirac peak containing all the mass (for  $D > 2$ ). This is not the structure obtained at  $t_{coll}$ . This implies that the evolution must continue in the post-collapse regime. The scenario that we are now exploring [21] is the following. A central Dirac peak containing a mass  $N_0(t)$  emerges at  $t > t_{coll}$ , whereas the density for  $r > 0$  satisfies a scaling relation of the form

$$\rho(r, t) = \rho_0(t) f\left(\frac{r}{r_0(t)}\right), \quad (48)$$

where  $\rho_0(t)$  is now decreasing with time (starting from  $\rho_0(t = t_{coll}) \rightarrow +\infty$ ) and  $r_0(t)$  grows with time (starting from  $r_0(t = t_{coll}) = 0$ ). As time increases, the residual mass for  $r > 0$  is progressively swallowed by the dense core made of particles which have fallen on each other. It is the purpose of the rest of this paper to show that this scenario actually holds, as well as to obtain analytical and numerical results illustrating this final collapse stage.

For  $T = 0$ , the dynamical equation for the integrated mass  $M(r, t)$  reads

$$\frac{\partial M}{\partial t} = \frac{1}{r^{(D-1)}} M \frac{\partial M}{\partial r}, \quad (49)$$

with boundary conditions

$$M(0, t) = N_0(t), \quad M(1, t) = 1. \quad (50)$$

We define  $\rho_0$  such that for small  $r$

$$M(r, t) - N_0(t) = \rho_0(t) \frac{r^D}{D} + \dots \quad (51)$$

Up to the geometrical factor  $S_D^{-1}$ ,  $\rho_0(t)$  is the central residual density (the residual density is defined as the density after the central peak has been subtracted). For  $r = 0$ , Eq. (49) leads to the evolution equation for  $N_0$

$$\frac{dN_0}{dt} = \rho_0 N_0. \quad (52)$$

As  $N_0(t) = 0$  for  $t \leq t_{coll}$ , and since this equation is a first order differential equation, it looks like  $N_0(t)$  should remain zero for  $t > t_{coll}$  as well. However, since  $\rho_0(t_{coll}) = +\infty$ , there is mathematically speaking no global solution for this equation and non zero values for  $N_0(t)$  can emerge from Eq. (52), as will soon become clear.

We then define

$$s(r, t) = \frac{M(r, t) - N_0(t)}{r^D}, \quad (53)$$

which satisfies

$$\frac{\partial s}{\partial t} = \left(r \frac{\partial s}{\partial r} + Ds\right) s + \frac{N_0}{r^D} \left(r \frac{\partial s}{\partial r} + Ds - \rho_0\right). \quad (54)$$

By definition, we have also  $s(0, t) = \rho_0(t)/D$ .

We now look for a scaling solution of the form

$$s(r, t) = \rho_0(t) S\left(\frac{r}{r_0(t)}\right), \quad (55)$$

with  $S(0) = D^{-1}$  and

$$\rho_0(t) = r_0(t)^{-\alpha}, \quad (56)$$

where  $r_0$  is thus defined without ambiguity. Inserting this scaling *ansatz* in Eq. (54), and defining the scaling variable  $x = r/r_0$ , we find

$$\frac{1}{\alpha\rho_0^2} \frac{d\rho_0}{dt} (\alpha S + xS') = S(DS + xS') + \frac{N_0}{\rho_0 r_0^D} \frac{1}{x^D} (DS + xS' - 1). \quad (57)$$

Imposing scaling, we find that both time dependent coefficients appearing in Eq. (57) should be in fact constant. We thus define a constant  $\mu$  such that

$$N_0 = \mu\rho_0 r_0^D. \quad (58)$$

Equation (57) implies that  $\rho_0 \sim (t - t_{coll})^{-1}$ , which along with Eq. (56) implies that  $N_0 \sim (t - t_{coll})^{D/\alpha-1}$ . We thus find a power law behavior for  $N_0$ , which in order to be compatible with Eq. (52), leads to

$$\rho_0(t) = \left( \frac{D}{\alpha} - 1 \right) (t - t_{coll})^{-1}. \quad (59)$$

We end up with the scaling equation

$$\frac{1}{D-\alpha} (\alpha S + xS') + S(DS + xS') + \mu x^{-D} (DS + xS' - 1) = 0. \quad (60)$$

From Eq. (60), we find that the large  $x$  asymptotics of  $S$  is  $S(x) \sim x^{-\alpha}$ . In a short finite time after  $t_{coll}$ , it is clear that the large distance behavior of the density profile ( $r \gg r_0$ ) cannot dramatically change. We deduce that the decay of  $S$  should match the behavior for time slightly less than  $t_{coll}$  for which  $S(x) \sim x^{-\frac{2D}{D+2}}$ . Hence the value of  $\alpha$  should remain unchanged before and after  $t_{coll}$ . Finally, we obtain the following exact behaviors for short time after  $t_{coll}$ :

$$\rho_0(t) = \frac{D}{2} (t - t_{coll})^{-1}, \quad (61)$$

$$r_0(t) = \left( \frac{2}{D} \right)^{\frac{D+2}{2D}} (t - t_{coll})^{\frac{D+2}{2D}}, \quad (62)$$

$$N_0(t) = \mu \left( \frac{2}{D} \right)^{\frac{D}{2}} (t - t_{coll})^{\frac{D}{2}}. \quad (63)$$

We note the remarkable result that the central residual density  $\rho(0, t) = S_D^{-1} \rho_0(t)$  displays a universal behavior just after  $t_{coll}$ , a result already obtained in [20]. Moreover, we find that  $N_0(t)$  has the same form as the mass found within a sphere of radius  $r_0(t)$  below  $t_{coll}$ , given in Eq. (28).

Moreover, the scaling function  $S$  satisfies

$$\frac{D+2}{D^2} \left( \frac{2D}{D+2} S + xS' \right) + S(DS + xS') + \mu x^{-D} (DS + xS' - 1) = 0. \quad (64)$$

The constant  $\mu$  is determined by imposing that the large  $r$  behavior of  $s(r, t)$  (or  $\rho(r, t)$ ) exactly matches (not simply proportional) that obtained below  $t_{coll}$ , which depends on the shape of the initial condition as shown in [20]. Equation (64) can be solved implicitly

by looking for solutions of the form  $x^D = z[S(x)]$ . After cumbersome but straightforward calculations, we obtain the implicit form

$$1 + \frac{x^D}{\mu} S(x) = \left[ 1 + \frac{x^D}{\mu} \left( S(x) + \frac{2}{D^2} \right) \right]^{\frac{D}{D+2}}, \quad (65)$$

which coincides with the implicit solution given in [20]. Note that  $S(x)$  is a function of  $x^D$ . We check that the above result indeed leads to  $S(0) = D^{-1}$ , and to the large  $x$  asymptotics

$$S(x) \sim \mu^{\frac{2}{D+2}} \left( \frac{2}{D^2} \right)^{\frac{D}{D+2}} x^{-\frac{2D}{D+2}}. \quad (66)$$

Note finally that for  $T = 0$ ,  $N_0(t)$  saturates to 1 in a finite time  $t_{end}$ , corresponding to the deterministic collapse of the outer mass shell initially at  $r = 1$ . Indeed, using the Gauss theorem, the position of a particle initially at  $r(t = 0) = 1$  satisfies

$$\frac{dr}{dt} = -r^{-(D-1)}. \quad (67)$$

The position of the outer shell is then

$$r(t) = (1 - Dt)^{1/D}, \quad (68)$$

which vanishes for  $t_{end} = D^{-1}$ .

- *Post-collapse scaling at  $T > 0$*

In the more general case  $T \neq 0$ , we will proceed in a very similar way as in the previous section. We define again,

$$s(r, t) = \frac{M(r, t) - N_0(t)}{r^D}, \quad (69)$$

where  $N_0$  still satisfies

$$\frac{dN_0}{dt} = \rho_0 N_0. \quad (70)$$

We now obtain

$$\frac{\partial s}{\partial t} = T \left( \frac{\partial^2 s}{\partial r^2} + \frac{D+1}{r} \frac{\partial s}{\partial r} \right) + \left( r \frac{\partial s}{\partial r} + Ds \right) s + \frac{N_0}{r^D} \left( r \frac{\partial s}{\partial r} + Ds - \rho_0 \right). \quad (71)$$

By definition, we have again  $s(0, t) = \rho_0(t)/D$ .

We look for a scaling solution of the form

$$s(r, t) = \rho_0(t) S \left( \frac{r}{r_0(t)} \right), \quad (72)$$

with  $S(0) = D^{-1}$ . As before, we define the King's radius by

$$r_0 = \left( \frac{T}{\rho_0} \right)^{1/2}. \quad (73)$$

For  $t < t_{coll}$ , we had  $s(r, t) \sim 4Tr^{-2}$  (or  $S(x) \sim 4x^{-2}$ ). In a very short time after  $t_{coll}$ , this property should be preserved, which implies that the post-collapse scaling function should also behave as

$$S(x) \sim 4x^{-2}, \quad (74)$$

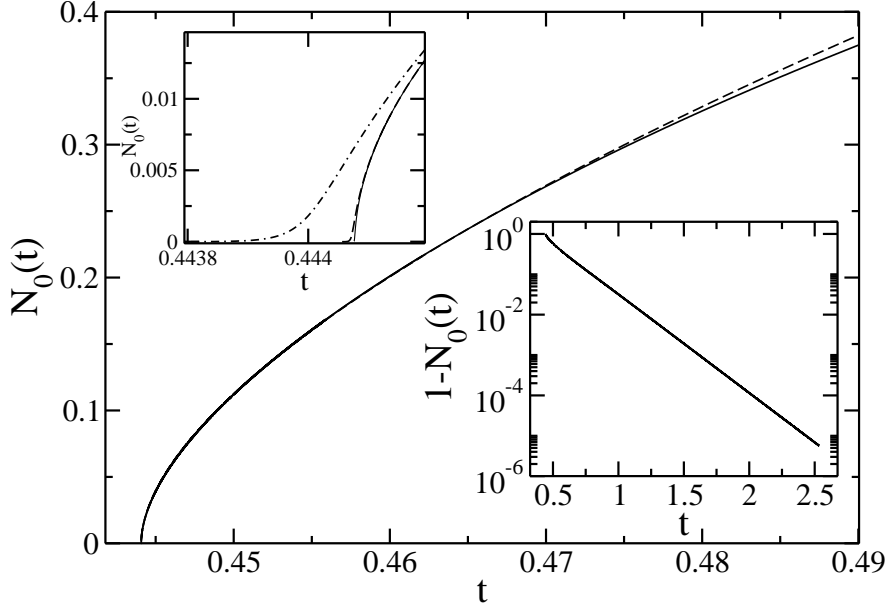


Figure 6: We plot  $N_0(t)$  for small time (full line). This is compared to  $N_0(t)^{\text{Theory}} \times [1 + a(t - t_{\text{coll}})^b]$  (dashed line), where  $N_0(t)^{\text{Theory}}$  is given by Eq. (80) with  $\mu = 8.38917147\dots$ , and  $a \approx 1.7$ . and  $b \approx 0.33$  are fitting parameters. Note that the validity range of this fit goes well beyond the estimated  $t_*$  with  $t_* - t_{\text{coll}} \sim T^{D/2} \sim 0.09$ . The bottom insert illustrates the exponential decay of  $1 - N_0(t) \sim e^{-\lambda t}$ . The best fit for  $\lambda$  leads to  $\lambda \approx 5.6362$  to be compared to the eigenvalue computed by means of Eq. (83),  $\lambda = 5.6361253\dots$ . Finally, the top inset illustrates the sensitivity of  $N_0(t)$  to the space discretization  $dx$ , which introduces an effective cut-off necessary in order to smoothly cross the singularity at  $t = t_{\text{coll}}$  (a factor 4 in  $dx$  between each of the 3 curves). Note the small time scale : even the curve corresponding to the coarsest discretization becomes indistinguishable from the others for  $t > 0.448$ .

for large  $x$ . Inserting the scaling *ansatz* in Eq. (71), we obtain

$$\frac{1}{2\rho_0^2} \frac{d\rho_0}{dt} (2S + xS') = S'' + \frac{D+1}{x} S' + S(DS + xS') + \frac{N_0}{\rho_0 r_0^D} \frac{1}{x^D} (DS + xS' - 1). \quad (75)$$

Again, this equation should be time independent for scaling to hold, which implies that there exists a constant  $\mu$  such that

$$N_0 = \mu \rho_0 r_0^D. \quad (76)$$

This leads to the universal behavior

$$\rho_0(t) = \left( \frac{D}{2} - 1 \right) (t - t_{\text{coll}})^{-1}. \quad (77)$$

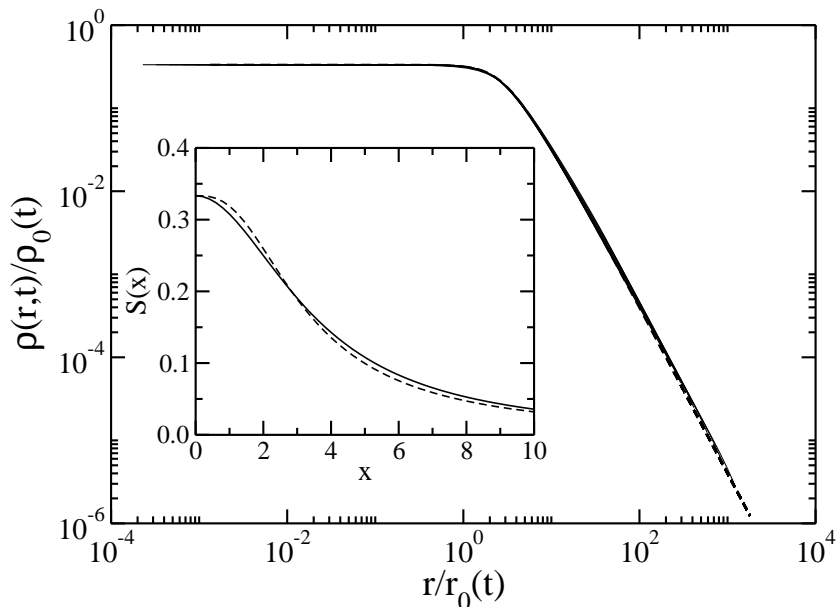


Figure 7: In the post-collapse regime, we plot  $\rho(r,t)/\rho_0(t)$  as a function of the scaling variable  $x = r/r_0(t)$ . A good data collapse is obtained for central residual densities in the range  $10^3 \sim 10^6$ . This is compared to the numerical scaling functions computed from Eq. (78) (dashed line). The insert shows the comparison between this post-collapse scaling function (dashed line) and the scaling function below  $t_{coll}$  which has been rescaled to have the same value at  $x = 0$ , preserving the asymptotics:  $S(x) = (3 + x^2/4)^{-1}$  (see Eq. (21); full line). Note that the post-collapse scaling function is flatter near  $x = 0$ , as  $S(x) - 1/3 \sim x^3$  (in  $D = 3$ ) instead of  $S(x) - 1/3 \sim x^2$ , below  $t_{coll}$ .

We thus end up with the scaling equation

$$\frac{1}{D-2} (2S + xS') + S'' + \frac{D+1}{x} S' + S(DS + xS') + \mu x^{-D} (DS + xS' - 1) = 0, \quad (78)$$

where  $\mu$  has to be chosen so that  $S(x)$  satisfies the condition of Eq. (74). Its value must be determined numerically. Note that for small  $x$ , the pre-collapse scaling function satisfies  $S(x) - S(0) \sim x^2$ , whereas the post-collapse scaling function behaves as

$$S(x) - S(0) \sim x^D. \quad (79)$$

However, contrary to the  $T = 0$  case,  $S(x)$  is not purely a function of  $x^D$ .

Finally, we find that the weight of the central peak has a universal behavior for short time after  $t_{coll}$

$$N_0(t) = \mu \left( \frac{2}{D-2} \right)^{D/2-1} T^{D/2} (t - t_{coll})^{D/2-1}. \quad (80)$$

Note that  $N_0(t)$  behaves in a very similar manner to the mass within a sphere of radius



$r_0$  below  $t_{coll}$ , shown in Eq. (23). The behavior of  $N_0(t)$  is illustrated in Fig. 6, while the scaling regime is displayed in Fig. 7.

In addition, comparing Eq. (80) and Eq. (63), we can define again a post-collapse cross-over time between the  $T \neq 0$  and  $T = 0$  regimes

$$t_* - t_{coll} \sim T^{D/2}, \quad (81)$$

which is similar to the definition of Eq. (29).

- *Large time limit for  $T > 0$*

For very large time, that is when almost all the mass has collapsed at  $r = 0$ , so that  $N_0(t) \approx 1$ , the residual density satisfies

$$\rho(r, t) \sim e^{-\lambda t} \psi(r), \quad (82)$$

where  $\psi$  satisfies the eigenequation

$$-\lambda \psi(r) = T \left( \psi'' + \frac{D-1}{r} \psi' \right) + \frac{1}{r^{D-1}} \psi'. \quad (83)$$

We did not succeed in solving analytically the above eigenequation, and for a given temperature, this has to be solved numerically. However, in the limit of very small temperature, we can apply techniques reminiscent from semiclassical analysis in quantum mechanics ( $T \leftrightarrow \hbar$ ). We now assume  $T$  very small and define  $h(r)$  such that

$$\psi(r) = \exp \left[ -\frac{\int_0^r h(x) dx}{T} \right]. \quad (84)$$

The function  $h$  satisfies the following non-linear first order differential equation

$$T \left( h' + \frac{D-1}{r} h \right) + \frac{h}{r^{D-1}} - h^2 = \lambda T, \quad (85)$$

with the simple boundary condition

$$h(1) = 1. \quad (86)$$

In the limit  $T \rightarrow 0$ , the term proportional to  $T$  in the left-hand side of Eq. (85) can *a priori* be discarded leading to [21]

$$h(r) = \frac{2\lambda T r^{D-1}}{1 + \sqrt{1 - 4\lambda T r^{2(D-1)}}}, \quad (87)$$

which is valid for  $1 - r \gg T^{2/3}$ . Solving perturbatively Eq. (85) leads to

$$\lambda = \frac{1}{4T} + \frac{c_D}{T^{1/3}} + \dots \quad (T \rightarrow 0), \quad (88)$$

where  $c_D$  is a  $D$  dependent constant.

In the inverse formal limit of large temperature (although in practice  $T < T_c$ ), we obtain

$$\lambda = D + \frac{D^2}{2(D+2)} \frac{1}{T} + \dots \quad (T \rightarrow +\infty). \quad (89)$$

The results of Eq. (88) and Eq. (89) are illustrated on Fig. 8.

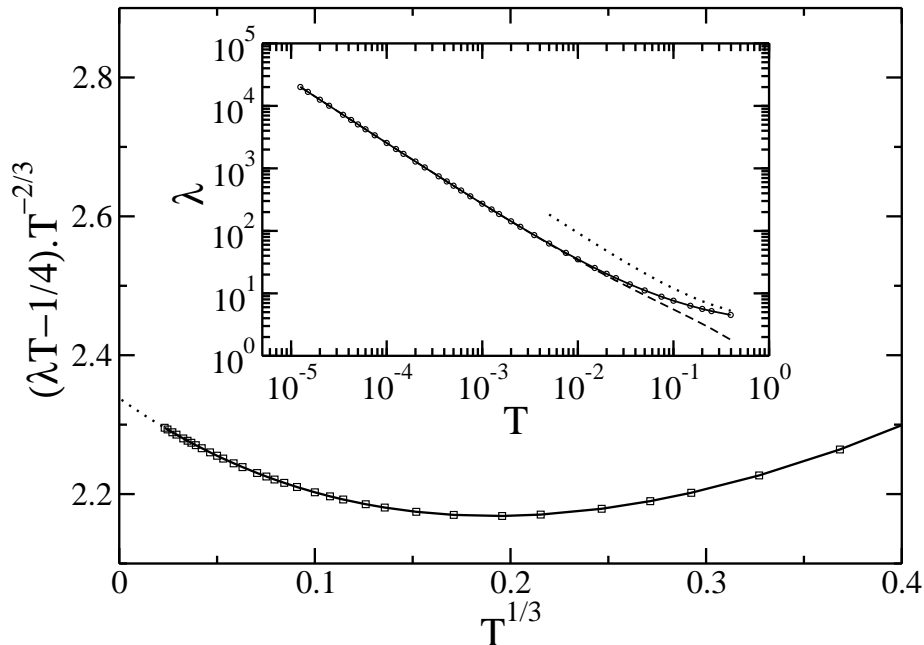


Figure 8: We plot  $\lambda$  as a function of temperature (insert). The dashed line is the small temperature expansion of Eq. (88), whereas the dotted line is the large temperature estimate which is not very accurate in the physically relevant region  $T < T_c$ . The main plot represents  $(\lambda T - \frac{1}{4}) T^{-2/3}$  as a function of  $T^{1/3}$  (line and squares), which should converge to  $c_{D=3} = 2.33810741\dots$  according to Eq. (88). We find a perfect agreement with this value using a quadratic fit (dotted line).

#### 4. Conclusion

In this paper, we have illustrated the rich properties of a Brownian model of gravitational collapse in both canonical and microcanonical ensembles. Quantitative results have been obtained for any dimension of space  $D \geq 2$  (including the critical dimension  $D = 2$ ) and any temperature  $T \leq T_c$  (including the peculiar case  $T = 0$ ). In the microcanonical ensemble, we have shown that although the scaling equation possesses solutions corresponding to  $\alpha > 2$ , the solution with  $\alpha = 2$  ultimately prevails. However, we have argued that in a model for which the temperature is not kept uniform, we should expect a value of  $\alpha$  greater than 2 to be selected. In the canonical ensemble, we have also shown that the singular point  $t = t_{coll}$  is not the final state of the dynamics, which is consistent with thermodynamical considerations which predicts a totally condensed state at  $r = 0$  at equilibrium [14, 5]. We have investigated this post-collapse regime analytically, which displays backward scaling solutions. Finally, using semiclassical methods, we have described the very large time regime analytically. Note that the post-collapse regime in

the microcanonical ensemble is more complex. It is marked by the formation of a central body with small mass and small radius but with huge potential energy. This structure is reminiscent of a “binary star” in astrophysics. It is surrounded by a very hot halo with  $T \rightarrow +\infty$  that is almost homogeneous. This “binary-halo” structure is the most probable structure in the microcanonical ensemble as its entropy  $S \sim \ln T \rightarrow +\infty$  [20]. Thus, it should be reached in the post collapse regime. However, the Smoluchowski-Poisson system becomes ill-defined as  $T = \infty$  so that the evolution of the system after  $t_{coll}$  is pathological and requires a small-scale regularization [21]. When a small-scale cut-off  $h$  is introduced, it is found that the mass of the core decreases as  $h$  decreases while the temperature increases. This corroborates the previous qualitative discussion and gives a hint as to how a rigorous description of the post-collapse regime could be undertaken.

Except for some exact results, most of our analytical results have been obtained by perturbative (Eq. (88), Eq. (89),...) or non perturbative methods (Eq. (46), Eq. (47),...). We hope that mathematicians will find the following problems interesting to study in a more rigorous way.

- Concerning the microcanonical collapse scaling equation, it would be interesting to justify the existence of the function  $\alpha[S(0)]$  (or  $S(0)[\alpha]$ ), leading to a maximum value  $\alpha = \alpha_{max}$  for physical solutions.
- The correct mathematical definition of the post-collapse stage following the singular point  $t = t_{coll}$ , and the justification of our supposedly exact estimates for  $\rho_0(t)$  and  $N_0(t)$  are certainly needed.

## References

- [1] E. Abdalla and M.R. Tabar, Phys. Lett. B **440**, 339 (1998).
- [2] J. Binney and S. Tremaine, *Galactic Dynamics* (Princeton Series in Astrophysics, 1987).
- [3] P.H. Chavanis, Astron. Astrophys. **356**, 1089 (2000).
- [4] P.H. Chavanis, in: *Dynamics and thermodynamics of systems with long range interactions*, edited by T. Dauxois, S. Ruffo., E. Arimondo and M. Wilkens, (Lecture Notes in Physics, Springer, 2002) [cond-mat/0212223].
- [5] P.H. Chavanis, Astron. Astrophys. **381**, 340 (2002).
- [6] P.H. Chavanis, Phys. Rev. E **68**, 036108 (2003).
- [7] P.H. Chavanis and C. Sire, Phys. Rev. E **69**, 016116 (2004).
- [8] P.H. Chavanis and C. Sire, Phys. Rev. E, in press [cond-mat/0402227].
- [9] P.H. Chavanis, M. Ribot, C. Rosier and C. Sire, this issue (2004) [cond-mat/0407386].
- [10] P.H. Chavanis, C. Rosier and C. Sire, Phys. Rev. E **66**, 036105 (2002).
- [11] P.H. Chavanis, J. Sommeria and R. Robert, Astrophys. J. **471**, 385 (1996).

- [12] I.A. Guerra, M.A. Peletier and J. Williams, preprint.
- [13] E. Keller and L.A. Segel, *J. theor. Biol.* **26**, 399 (1970).
- [14] M. Kiessling, *J. Stat. Phys.* **55**, 203 (1989).
- [15] D. Lynden-Bell and R. Wood, *MNRAS* **138**, 495 (1968).
- [16] J.D. Murray, *Mathematical Biology* (Springer, 1991).
- [17] T. Padmanabhan, *Phys. Rep.* **188**, 285 (1990).
- [18] H. Risken, *The Fokker-Planck equation* (Springer, 1989).
- [19] R. Robert and J. Sommeria, *Phys. Rev. Lett.* **69**, 277 (1992).
- [20] C. Sire and P.H. Chavanis, *Phys. Rev. E* **66**, 046133 (2002).
- [21] C. Sire and P.H. Chavanis, *Phys. Rev. E* **69**, 066109 (2004).